

28 a 31 de maio de 2017 | Brasília/DF  
www.sobrac2017.com.br

## **Construção de bancada de testes para estudos de ruído de jatos aplicados ao ruído aeronáutico**

COELHO, Eduardo L.C.<sup>1</sup>; DESCHAMPS, César J.<sup>2</sup>, CORDIOLI, Julio A.<sup>2</sup>, LAUTERJUNG Q., Rudner<sup>1</sup>, BASTOS, Leopoldo<sup>2</sup>, SIROTTO, José R. N.<sup>2</sup>, CARMO, Micael G. V.<sup>1</sup>, CATALANO, Fernando M.<sup>3</sup>.

(1) Embraer SA; (2) Universidade Federal de Santa Catarina; (3) Escola de Engenharia de São Carlos da USP.

### **RESUMO**

Este trabalho apresenta a Bancada de Ruído de Jatos desenvolvida pela UFSC e seus parceiros no âmbito do Projeto Aeronave Silenciosa Fase 2 – Desenvolvimento de Soluções Aprimoradas para o Problema de Ruído Externo (2012-2015). São expostas as principais funcionalidades da bancada e soluções de projeto adotadas. A seção de testes e planta de ar comprimido foram projetadas para receber bocais de diferentes geometrias e tamanhos, além de produzir uma ampla faixa de velocidades de jato subsônicas para um bocal de no mínimo 5 cm. Um arco de microfones foi instalado para medições simultâneas de campo afastado em diferentes ângulos de observação. Segundo o processo de validação acústica pode-se garantir uma boa relação sinal-ruído, bem como características anecóicas satisfatórias para a câmara de testes. A capacidade de produzir jatos estáveis não aquecidos até Mach 0,9, com potencial de atingir regime supersônico também é demonstrada. Os resultados obtidos até agora para um bocal cônico padrão (SMC000) de 5 cm de diâmetro veem mostrando uma boa comparação (até 2 dB) com dados da literatura e de bancadas semelhantes.

**Palavras-chave:** ruído de jato.

### **ABSTRACT**

This work presents the Jet Noise Rig developed by UFSC and its partners during the Project Aeronave Silenciosa Phase 2. Some of its main functionalities and design tradeoffs are presented. The test section and compressed air plant were designed to receive different test nozzle sizes and shapes and producing several subsonic jet Mach number for at least a 2" diameter nozzle. An arc of microphones is available for simultaneous far field acoustic measurements. From its commissioning procedures it was confirmed that the facility has fairly reasonable signal to noise ratio and anechoic characteristics. It is demonstrated that it can provide unheated stable jets at up to Mach number 0.9, with the potential of increasing it to supersonic speeds. The acoustic results obtained so far for simple conic nozzle (SMC000) are in good agreement (within 2 dB) with similar facilities and the general trends expected in literature.

**Keywords:** jet noise.

## **1. INTRODUCTION**

Aircraft external noise levels have been reduced over last decades mainly due to technological improvements, implemented in aero-engines. However, the noise produced by the engine exhaust jet, and its interaction with airframe surfaces, are still a major issue in the certification

of modern commercial aircrafts or while operating at noise sensitive airports. Since experimental campaigns in industrial jet noise test facilities can be cost prohibitive for early conceptual design and research programs, a usual way to test preliminary concepts and validate prediction models is to run experiments in smaller scale facilities. These so called “jet rigs” are built in order to run measurements of turbulent jet features in a controlled laboratory environment.

The aeroacoustic mechanisms of jet noise can be briefly described by the development of turbulent eddies convecting through the shear layer present in the jet interface with the ambient air interacting with each other producing pressure fluctuations that can propagate to far observers by means of sound waves. Whether such mechanisms are essentially stochastic (BILSON et al., 2003) or not (CAVALIERI et al., 2013) is something that is being intensely studied. But what most researchers seem to agree is that the whole jet plume volume contributes for creating a complex aeroacoustic source which is non compact and continuously distributed. Such properties are responsible for producing very special and easily recognizable broadband spectra and directivity patterns. For flow speeds greater than the local speed of sound, shock cell phenomena will also appear affecting significantly the acoustic signature of the jet. Figure 1 is a compilation from several references and it summarizes the jet noise mechanisms, some typical spectra and how the introduction of coaxial jets with secondary bypass flow affects engine exhaust noise and consequently the aviation industry.

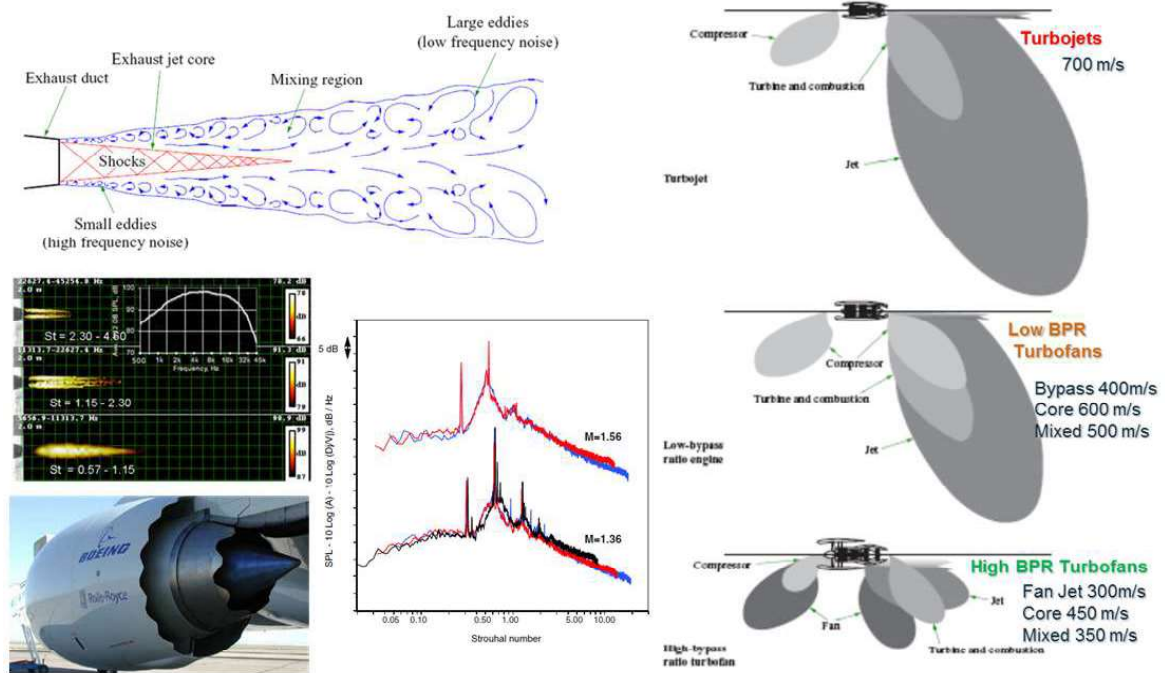


**Figure 1:** Typical jet noise features and applications in aviation industry. Sources: ESDU (2002), Viswanathan (2008), Nesbitt (2007)

This work focuses on the design and acoustic validation of a jet noise rig recently built at the Laboratory of Acoustic and Vibration (LVA), Federal University of Santa Catarina (UFSC). To this aim, a brief description of the rig project is provided, together with results from noise measurements at LVA’s jet rig, which are compared with experimental data available in the literature. Prior to the jet noise measurements, a detailed analysis was performed to investigate relevant parameters that could affect the measurements, such as the acquisition system, facility control, jet stability, flow properties, positioning of microphones and background noise due to machinery. The isolated jet validation tests were run for a smooth

circular nozzle with 2" diameter, cold flow and subsonic conditions (Mach number 0.3 to 0.9). The nozzle geometry used is the same as the series of NASA Small Metal Chevrons. Results for a single jet indicated that LVA/UFSC jet noise rig can be considered acoustically validated, since the sound field measured is in agreement with published data and expected trends.

## 2. DESIGNING A JET RIG

### 2.1 Facility Description

The jet noise rig at LVA/UFSC consists of the following elements: a compressed air line, a plenum, a discharge nozzle, an anechoic chamber, a flow control system and an acoustic data acquisition system. A schematic of the rig is shown in Figure 1. The compressed air line is constituted, in order, by: compressor, filters for particulate removal, two-towered dehumidifier to guarantee a dry air flow, a first check valve to block air from returning in the line, pressure vessel for air storage, a second check valve and a flow control valve. The air that exits the control valve is discharged in the plenum (a smaller pressure vessel which works as a settling chamber with special acoustic treatment in its interior). The purpose of this device is to remove the noise generated by the upstream airflow and other plant machinery, and it is also admitted as a stagnation condition for the fluid. Upon exiting the plenum, the air follows a 6" diameter line until it finds a convergent nozzle.

The storage tank of 15 m<sup>3</sup> operates with Maximum Working Pressure (MAWP) of 12.5 bar and it is installed outside the building. The air is pressurized by a rotary single staged screw compressor that operates at up to 10.5 m<sup>3</sup> / min with Maximum Working Pressure of 12.8 bar. Before reaching the tank, the air passes through a filtering system and gets dehumidified by a dryer (dew point down to -40° C). The internal chamber volume with acoustic treatment is approximately 60 m<sup>3</sup>, with 5 m long, 4.05 m high and 2.95 wide (see scheme in Figure 2).

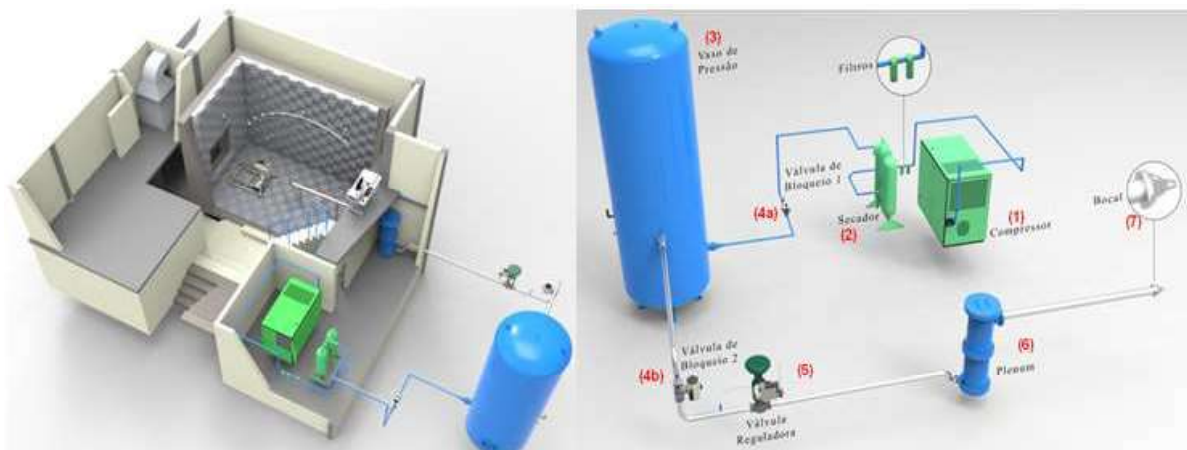


**Figure 2:** Scheme of LVA's jet rig including the compressed air line and test chamber. Source: Bastos (2016)

### 2.2 Design Requirements and Trade offs

One of the greatest challenges in the design of this facility was to fit it into a previously built infra-structure with very limited space. Some more difficulties arise when the surrounding area is a densely occupied university campus with safety and environmental restrictions. The electric power supply had to be upgraded to over 100 kVA during the civil constructions for supporting the power demand from the compressor and other rig exclusive hardware.



**Figure 3:** Location of the UFSC Jet Rig. Source: Google Maps (modified)

First estimates pointed that the acoustic room available, which couldn't be expanded, barely fit to the farfield criteria recommended by AHUJA (2003) and VISWANATHAN (2008). So a simplified “chamber design calculator” had to be developed in order to assess the tradeoff between the main design parameters and checking their compliance with critical requirements. Table 1 summarizes how such parameter cross relate.

**Table 1:** Design Parameters and Requirements

Design Parameters	Design Point, Requirements	Other Technical Restrictions
<ul style="list-style-type: none"> <li>•Target nozzle scaling factor and rig design diameter</li> <li>•scale frequency ranges for microphone selection and chamber cut on frequency</li> <li>•microphone arc position</li> <li>•acoustic absorbent thickness and material properties</li> <li>•size of “air briefing” vents to be cut on chamber walls</li> </ul>	<ul style="list-style-type: none"> <li>•To Produce a stable Single cold jet up to Acoustic Mach 0.9 (<math>V_{jet}/c_0</math>) for at least 30 sec</li> <li>•To measure acoustic farfield within a polar angle range of <math>60^\circ</math> to <math>150^\circ</math></li> <li>•To cover a frequency range equivalent to real scale limits of 50 Hz and 12,5 kHz</li> <li>•To measure relevant spectra for target real scale nozzle from 0.5 to 1.5 m diameter</li> </ul>	<ul style="list-style-type: none"> <li>•Microphone to acoustic treatment minimum distance</li> <li>•Acoustic treatment (wedges or not) thickness for satisfying 1/4th lambda criteria for cut on absorption</li> <li>•Minimum flow recirculation inside chamber due to free air entrainment into the jet</li> <li>•Chamber dimensions fixed and limited space for compressed air plant</li> <li>•Minimum impact on campus life and community noise</li> </ul>

Other important characteristics are associated with jet flow properties such as jet plume symmetry and stability over time and velocity profile consistency with potential core theory. Most of it is related to the compressed air capacity and control but also depends on a good behavior of the free air entrainment into the jet. Regarding the last effect some preliminary CFD simulation showed that the chamber layout (including the exhaust chamber downstream) have the potential to produce some low speed recirculation cells which could cause jet instabilities or induce low frequency noise and undesired vibration to the microphones. After several design iterations an optimized air vent location was found such that maximum air velocity in microphone region stayed below 1 m/s limit and mean flow jet stays symmetric.

After a few design interactions the team could decide for a reasonable tradeoff between air vents and exhaust chamber dimensions, jet nozzle position and acoustic treatment thickness

such that most criteria were satisfied. The dimensions of the wedges are 0.2 m long, 0.1 m wide and 0.3 m long and were installed alternating orientation in 3 wedges arrangements. This configuration imparts a cutoff chamber frequency of approximately 400 Hz. Regarding the microphone position AHUJA (2003) recommends a range of 45 to 70 nozzle diameters with respect to nozzle exit in order to assure farfield conditions.



**Figure 4:** Rig Test chamber with acoustic treatment and microphone arc for polar angle farfield measurements

Not only the chamber walls but also some building structures had to be cut or modified in order to receive the special equipment for the rig or simply to assure that the test section was acoustically isolated and without flow recirculation. Other counter measures for preventing noise pollution in other campus activities are still on their way.

### **2.3 Dimensioning and Controlling of the Compressed Air System**

Regarding the facility capacity a transient model was derived from isotropic relation from the storage tank to ultimate nozzle expansion so that the time test window could be assessed. It turns out that even without adding active flow control for refilling the vessel, the pressure and temperature drop during discharge was sufficient for handling aeroacoustic measurements. In other words a theoretic test window of 60 sec with a smooth jet velocity decay of 10% at critical design point was achieved.

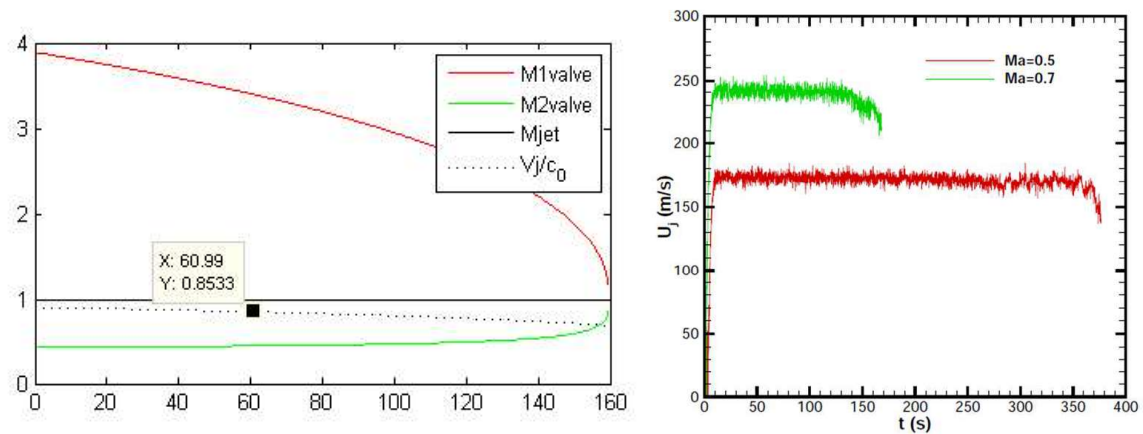


**Figure 5:** Isentropic analysis of jet velocity decay with time. Modeled (black curve, left) versus measured (right)

The flow control software is based on isentropic relations of the airflow using pressure and temperature values from both the plenum and the anechoic chamber measured at a 10 Hz acquisition rate. The software was designed to operate, monitor and control the experiments in the jet rig based on the setpoints defined by acoustic Mach number. From the virtual control panel it is possible to set the compressor working point and percentage of valves aperture. It also displays the real time acquired data from the pressure and temperature sensors, placed in the chamber, the plenum and monitors the inlets and outlets of the compressed air plant as well. The information from the sensors is then used to calculate the Mach number based on an isentropic flow relation given below. Figure 6 shows the software front panel. The elements circled in red are the one which belong to the pipeline, and the ones in blue are the elements of actuation and monitoring.

The flow control valve is the main control element of the software. Its percentage of aperture is displayed on the interface, varying from 0% (completely opened) and 100% (completely shut). If the automatic mode is on, the percentage of aperture becomes a mere indicator as it changes in order to achieve the Mach number desired. The user may also use a fixed aperture, in which case this parameter can be set at any time. The interface also shows the pressure and temperature at the plenum and the chamber and the jet velocity that corresponds to the Mach number set on the automatic mode.

In order to exemplify the proper functioning of the algorithm, Figure 6 shows the jet velocity provided by the control software as a function of time for the conditions  $Ma=0.5$  and  $Ma=0.7$ , which were the conditions used in the experiments described below. It may be verified that the mean velocity corresponding to each Mach number was successfully kept constant for a considerable length of time. For  $Ma=0.5$ , the velocity was kept constant for nearly 350s, which gives a 6 min time window for the aerodynamic tests. For the  $Ma=0.7$  condition, the time window is 140s. It may be observed that the jet velocity oscillated around the mean value, due to the high rate of actuation chosen (the loop was performed every 0.1s). Nevertheless, the mean value was controlled properly, providing good conditions for the aerodynamic and acoustic tests.

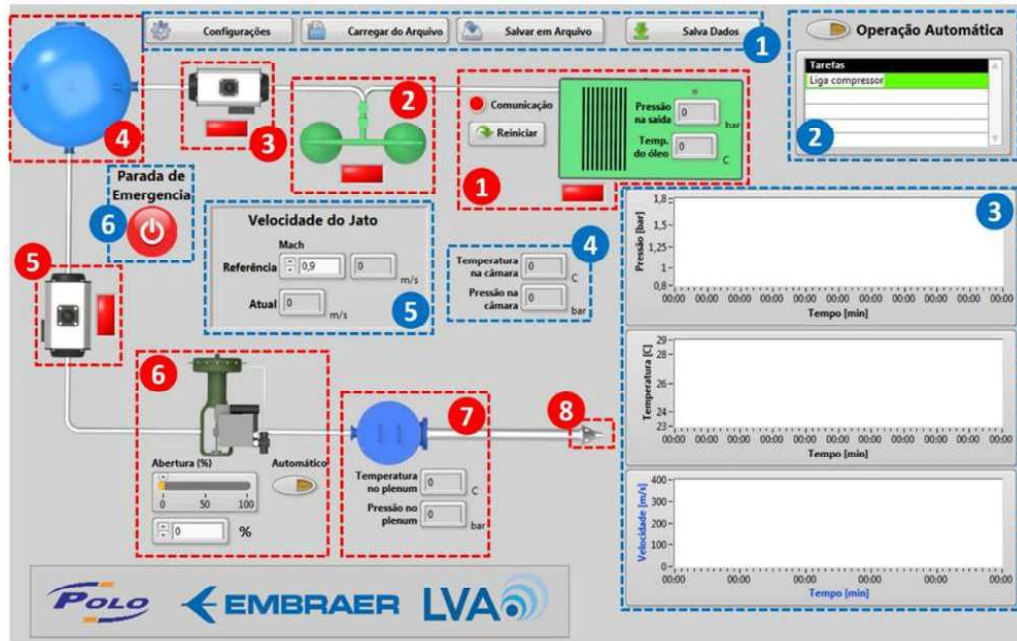


Figure 6: The Flow Control Software Interface (left) and measured Rig velocity profiles (right).

## 2.4 Acoustic Acquisition System

The acoustic data acquisition system is composed of 10 1/4" free field microphones (G.R.A.S. Type 42BE) with working frequency range of 10 to 100 kHz, and a PXIe platform model 1082 from Nation Instruments (NI). Allocated to the PXIe platform are two PXIe 4499 data acquisition cards and a PXI 6723 static and waveform analogue output card, both manufactured by NI. The commercial data acquisition and signal processing software Signal Express (NI) was used. The microphones are allocated over an arc of 2.1 m radius and covering 60° to 150° angles from the jet axis, with 150° being upstream the nozzle and 60° downstream. Acoustic measurements last around 20 s with a sampling frequency of 120 kHz and the results being an average of 200 samples for 1/3 octave bands and 1,000 samples for narrow-band. Both averages are linear and utilize Hanning window, while the narrow-band spectra also using a 50% overlap, which gives a 50 Hz band spacing.

In order to define the frequency range in which the system response is planar within acceptable errors. A similar methodology to the one adopted here was described in [3]. The methodology consists in generating a white noise in the same spectral frequency used by the data acquisition, and measuring the frequency response of the DAQ. The PXI-6723 card plugged to the PXIe platform and controlled by the Signal Express software is used to generate the white noise. The PXI-6723 is plugged to a connector block SCB-68A (NI), which directly sends the signal to the PXI-4499 (NI) data acquisition board. The PXI-4499 (NI) data acquisition board is the same used in the acoustics measurements and uses the same configurations: 20 s measurements with a 120 kHz sampling frequency and 50 Hz frequency resolution. Figure 2 displays the measured data in blue and a fitted curve in red. Without the oscillations found in the measured data, the fitted curve is utilized for analysis. It can be seen that the DAQ system has a practically flat response with deviations lower than 0.3 dB up until 55 kHz. Higher deviations above 55 kHz can be found, with values as high as 4 dB in 60 kHz. Distortions up to 0.3 dB are accepted, so that data will be acquired up to 50 kHz in narrow band, and the 1/3 octave band spectra will extend until 40 kHz (central frequency).

### 3. RIG VALIDATION

#### 3.1 Farfield Condition Evaluation

The position of the microphones is a vital aspect of the measurements, since the microphones may be positioned either at near field or the far field generated by jet noise. The interest lies in evaluating the source at the far field, where the particle velocity is in phase with the sound pressure and there is a 6 dB decay in the sound pressure level (SPL) per doubling of distance (assuming spherical propagation). The farfield condition was then verified for several Acoustic Mach numbers. The analysis was carried out at 4 angular positions (60°, 90°, 120° and 150°) and 6 distances from the nozzle center, ranging from 1.60 m to 2.10 m. For a 2" (0.0508 m) diameter nozzle the radial position to effective nozzle diameter ratio is ranging from approximately 32 (1.60 m) to 42 (2.10 m) diameters. Measurements were conducted 5 times for each Mach condition and an atmospheric attenuation function (ARP 866) was used to correct the data due to atmospheric absorption. The farthest position is assumed to be in the far field, and the inverse square law is drawn from this point including a +/- 0.5 dB margin of error, as show in Figure 7.

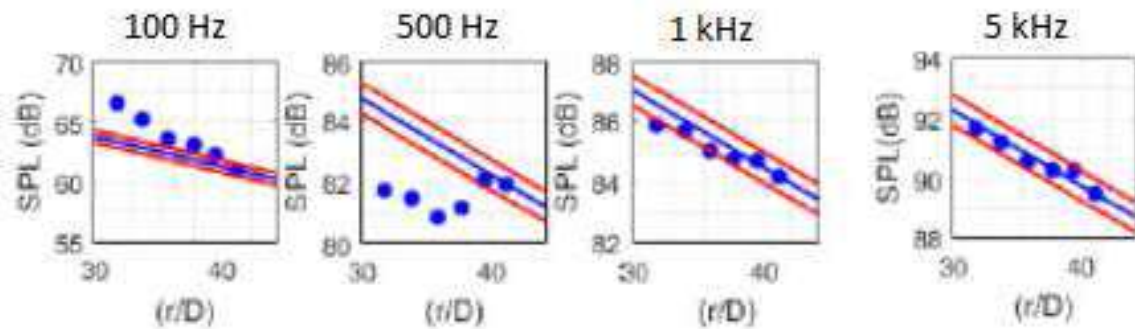


**Figure 7:** Farfield check for increasing distance from nozzle center ( $r/D$ ) at 0.9 Mach number and a 90° observer

Based on all test data, the farfield condition is considered to be achieved at all angular positions for frequencies above 500 Hz and a radial distance of 2.00 m (39 De). For precaution it was opted to allocate the microphones to a 2.10 m (42 De) radial distance. Apart from establishing the position of the microphones, this test also sets the lower frequency limit.

#### 3.2 Background Noise Evaluation

A methodology to assess the influence of rig and background noise is proposed. In this sense, background noise is assumed as the noise measured by the microphones when no flow is being released, while rig noise is the noise generated by the rig during its operation, excluding the jet noise. The proposed methodology is based on maintaining the same air mass flow rate in the compressed air line, while the discharge speed of the jet is considerably reduced by removing the nozzle. Therefore, the noise generated by the compressed air line is unaltered, while the jet noise is reduced so that the rig noise prevails. The SMC000 nozzle has an effective radius of 1" (0.0254 m) and the piping which it is nozzle is connected to, has a 3" (0.0762 m) effective radius, leading to a 9 times increase in terms of exhaust plane area.

Figure 8 shows the measured SPL in 1/3 octave bands between 500 Hz and 40kHz for 60°, 90° and 150° angular positions with the SMC000 nozzle installed and uninstalled. It is easily noticed that rig noise is well below the jet noise measured with the nozzle. It is possible to



state, then, that rig noise does not significantly affects the measure jet noise within the frequency range of interest.

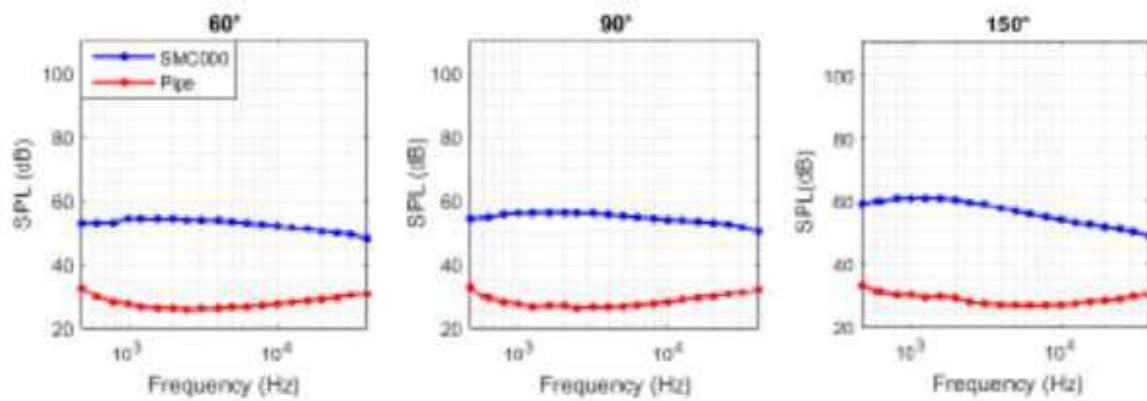


**Figure 8:** Background Noise Evaluation. SPL from the SMC000 nozzle installed (blue) and uninstalled (red)

### 3.3 Repeatability Check

In order to verify the repeatability of the measurements, 5 identical measurements were conducted in the same Mach number and the data distribution was analyzed. Figure 9 shows the results for several jet Mach numbers. The SPL deviations vary from 0.2 to 0.5 dB, while a deviation lower than 0.2 dB was observed at Mach 0.9. In general, it is expected that in the worst case scenario differences in the order of 0.5 dB would be seen.

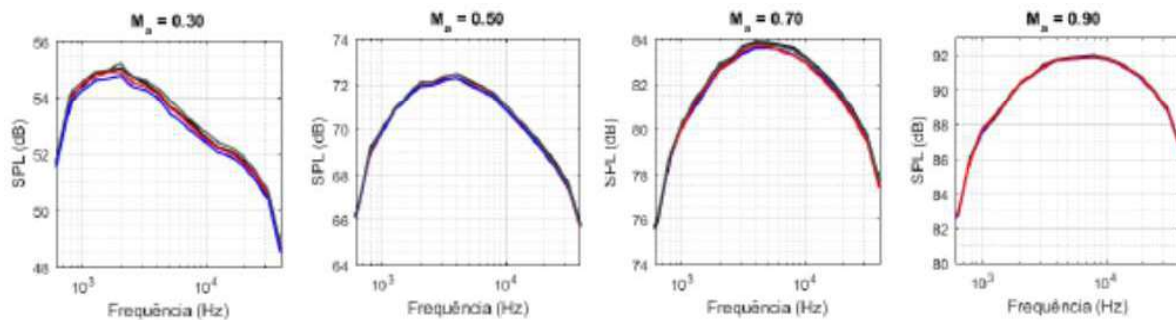


**Figure 9:** Repeatability Check of 1/3th OB SPL for several jet Mach numbers. Each curve is a different run

### 3.4 Validation with Benchmark Data

Figure 10 shows 1/3 octave results obtained at the LVA (UFSC) jet rig, together with measured data from Bridges & Brown (2005). Both data are shown from 500 Hz to 400 kHz 1/3 octave frequency band, without atmospheric absorption loss, following ARP 866 (1964) procedures, and scaled to 100De for comparison. For angular positions 60° to 120° the maximum deviation found between the data sets is less than 2 dB. For the angular position 150°, a maximum difference of 2 dB can be seen for frequencies higher than 1 kHz, but between the 500 Hz and 1 kHz frequency bands it is possible to notice a larger difference amongst higher velocity curves, although not greater than 4 dB.

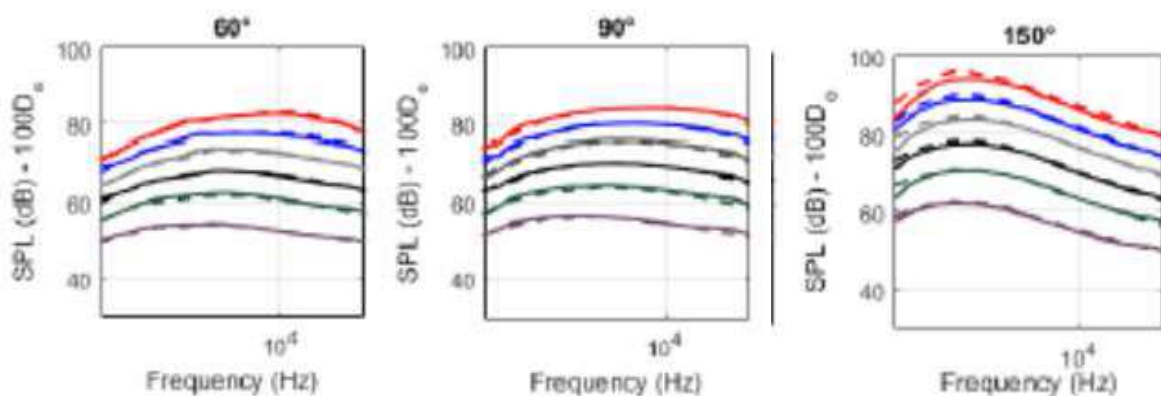


**Figure 10:** SPL Comparison of UFSC jet rig (solid curves) with Bridges & Brown (2005) (dashed) at several polar angles and Mach numbers 0.4 (purple), 0.5 (green), 0.6 (black), 0.7 (grey), 0.8 (blue) and 0.9 (red)

It can be considered that the measured noise levels at the LVA/UFSC jet noise rig are in accordance with the literature and that the few discrepancies found can be associated to experimental errors such as imprecision in the microphones' angular position and/or physically associated to the piping extension before the nozzle.

Further investigations, to be done on this Rig, will include different nozzle geometries and their interaction with near surfaces, being an interesting tool for Jet Noise research.

#### 4. REFERENCES

- AHUJA, K. K. **Designing Clean Jet Noise Facilities and Making Accurate Jet Noise Measurements**. AIAA Conference Paper 2003-0706, 2003.
- ARP. **Standard Values of Atmospheric Absorption as a Function of Temperature and Humidity**, ARP item 866, 1964.
- BASTOS, L. **Desenvolvimento e Emprego de uma Bancada para Análise de Efeitos de Instalação sobre Jatos de Bocais Serrilhados**. PhD Thesis, 2016 (in Portuguese).
- BILSON, M., ERIKSSON, L., DAVIDSON, L., **Jet Noise Prediction Using Stochastic Turbulence Modeling**. 9th AIAA/CEAS Aeroacoustics Conference and Exhibit, 2003.
- BRIDGES, J., BROWN, C. A., **Validation of the Small Hot Jet Acoustic Rig for Aeroacoustic Research**, AIAA Paper 2005-2846, 2005.
- CAVALIERI, A.V., RODRIGUEZ, D., JORDAN, P., COLONIUS, T., GERVAIS, Y. **Wavepackets in the velocity field of turbulent jets**. J. Fluid Mech. (2013), vol. 730, pp. 559–592, 2013.
- ESDU, **An Introduction to Aircraft Noise**, ESDU item 02020, ESDU International plc, London, 2002.
- GOOGLE MAPS: <https://www.google.com.br/maps>
- LIGHTHILL, M. J., **On Sound Generated Aerodynamically. I - General Theory**. Proceedings of the Royal Society of London, Series A, Mathematical and Physical Sciences, vol. 211, n° 1107, pp. 564-587, 1952.
- NESBITT, E., BRUNSNACK, L., UNDERBRINK, J., LYNCH, D., MARTINEZ, M., **Effects of Chevron on Engine Jet Noise Structure**, AIAA Aeroacoustic conference, AIAA 2007-3597, 2007.
- VISWANATHAN, K. **Does a Model-Scale Nozzle Emit the Same Jet Noise as a Jet Engine?** AIAA JOURNAL Vol. 46, No. 2, 2008.